



Molecular Crystals and Liquid Crystals

Publication details, including instructions for authors and subscription information:

<http://www.tandfonline.com/loi/gmcl20>

Electrical Characteristics of Wide Temperature Range Phase

Manoj Bhushan Pandey ^a, Ravindra Dhar ^b & Roman Dabrowski ^c

^a Physics Department, University of Allahabad, Allahabad, India

^b Physics Department, Ewing Christian College, Allahabad, India

^c Institute of Chemistry, Military University of Technology, Warsaw, Poland

Version of record first published: 05 Oct 2009

To cite this article: Manoj Bhushan Pandey, Ravindra Dhar & Roman Dabrowski (2009): Electrical Characteristics of Wide Temperature Range Phase, *Molecular Crystals and Liquid Crystals*, 509:1, 363/[1105]-377/[1119]

To link to this article: <http://dx.doi.org/10.1080/15421400903066091>

PLEASE SCROLL DOWN FOR ARTICLE

Full terms and conditions of use: <http://www.tandfonline.com/page/terms-and-conditions>

This article may be used for research, teaching, and private study purposes. Any substantial or systematic reproduction, redistribution, reselling, loan, sub-licensing, systematic supply, or distribution in any form to anyone is expressly forbidden.

The publisher does not give any warranty express or implied or make any representation that the contents will be complete or accurate or up to

date. The accuracy of any instructions, formulae, and drug doses should be independently verified with primary sources. The publisher shall not be liable for any loss, actions, claims, proceedings, demand, or costs or damages whatsoever or howsoever caused arising directly or indirectly in connection with or arising out of the use of this material.

Electrical Characteristics of Wide Temperature Range SmC_α^* Phase

Manoj Bhushan Pandey¹, Ravindra Dhar²,
and Roman Dabrowski³

¹Physics Department, University of Allahabad, Allahabad, India

²Physics Department, Ewing Christian College, Allahabad, India

³Institute of Chemistry, Military University of Technology,
Warsaw, Poland

We have studied a compound (S)-(+)-4-(1-methylheptyl) 4-[4-(3-hexanoyloxyprop-1-oxy)benzoyloxy]biphenylate by means of differential scanning calorimeter, polarizing microscope and dielectric spectroscopy. This compound shows exceptionally a wide temperature range of SmC_α^ phase $\sim 9^\circ\text{C}$ together with a paraelectric SmA^* phase. A relaxation mechanism in the high kHz region has been detected for the SmC_α^* phase under planar orientation of the molecules. This mechanism has been characterized with temperature and bias electric field. Recent theoretical advances predict two different nature of dielectric relaxation mode in the SmC_α^* phase (Phys. Rev. E, 69, 031709, 2004). Our experimental results confirm two different behaviors of this relaxation mode in different temperature range of the phase.*

Keywords: bias field dependence; chiral phases; dielectric permittivity and loss; dielectric relaxation; soft mode

PACS Number(s): 61.30.-v; 77.84.Nh; 64.70.Md

1. INTRODUCTION

The SmC_α^* phase is one of the subphases generally reported in anti-ferroelectric liquid crystal materials below paraelectric SmA^* phase.

MBP wish to thank Department of Science and Technology (DST), Government of India, New Delhi, India for financial assistance in the form of a fast track project (SR/FTP/PS-14/2005) to young scientist. The authors sincerely thank to Professor Pradip Kumar, Head, Physics Department and Professor I. M. L. Das, Physics Department, University of Allahabad, Allahabad for their support.

Address correspondence to Manoj Bhushan Pandey, Physics Department, University of Allahabad, Allahabad-211 002, India. E-mail: mbpandey@gmail.com

The discovery of this phase was associated with the discovery of anti-ferroelectric SmC_A^* phase in MHPOBC [1]. The structure of SmC_α^* phase has been determined to be incommensurate nano scale helical pitch extended from three to eight smectic layers [2,3]. In the dielectric spectrum of the SmC_α^* phase generally single relaxation mode in high kHz region is observed for planar oriented sample [4–8]. Origin of this mode is assigned to tilt fluctuation of molecules i.e., soft mode. In few materials this mode has been observed in low kHz region and its origin has been assigned to Goldstone mode [9]. A theoretical model have been proposed by Vaupotic *et al.* to explain the dielectric relaxation mechanism of SmC_α^* and other chiral smectic phases [10]. They have predicted two dielectric relaxation processes namely amplitude and phase fluctuation modes in the SmC_α^* phase. Recently we have reported two dielectric modes in the SmC_α^* phase of a Cl-MHPOBC compound [11]. We have demonstrated temperature and bias electric field dependence of two relaxation modes of the SmC_α^* phase in concurrence with the theoretical work of Vaupotic *et al.* Doualli *et al.* have extended the work of Vaupotic *et al.* by numerical simulation method which are supported by electro-optic and dielectric measurements [12]. We have verified the assumption of Doualli *et al.* in our recent work [13]. Since the details of the dielectric behaviour of SmC_α^* phase are still under discussion, accurate experimental data is needed to verify the proposed theoretical dielectric models [10,12]. The dielectric data are also important to ascertain the macroscopic electrical properties of this phase. So far, dielectric measurements turned out to be quite difficult, mostly because of the temperature range in which SmC_α^* phase exist is very narrow and usually does not exceed 1 K. Hence dielectric behaviour of SmC_α^* phase are also affected due to the adjacent low temperature phase [8]. There are very few systems showing SmC_α^* phase in the wide temperature range [4–7]. Recently Prof. Dabrowski group in Poland have synthesised (S)-(+)-4-(1-methylheptyl) 4-[4-(3-hexanoyloxyprop-1-oxy)benzoyloxy]biphenylate (molecular structure shown in Fig. 1) [14]. We found that compound shows exceptionally wide temperature range of SmC_α^* phase. In this work we are reporting dielectric properties of this compound with temperature, bias electric field and thickness of the sample.

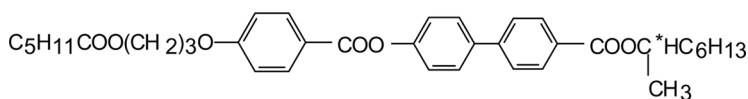


FIGURE 1 The molecular structure of investigated compound (S)-(+)-4-(1-methylheptyl) 4-[4-(3-hexanoyloxyprop-1-oxy)benzoyloxy]biphenylate.

2. THEORY

The theoretical formulas of the dielectric strength and the relaxation frequency of two modes in SmC_α^* phase are calculated by Vaupotic *et al.* which are following [10,12].

$$\Delta\varepsilon_P = \frac{K'}{2\pi f_P} \left(1 - \frac{2C(\alpha)}{2\pi\gamma(f_A - f_P)} \right) \quad (1)$$

$$\Delta\varepsilon_A = \frac{K'}{2\pi f_A} \left(1 + \frac{2C(\alpha)}{2\pi\gamma(f_A - f_P)} \right) \quad (2)$$

$$f_P/f_A = \frac{A(\alpha) + B(\alpha) \pm \sqrt{[A(\alpha) + B(\alpha)]^2 - 4[A(\alpha)B(\alpha) - C(\alpha)^2]}}{4\pi\gamma} \quad (3)$$

where,

$$A(\alpha) = a_0 + 3b_0\theta^2 + a_1 \cos^2(\alpha) + \frac{a_2}{4} \cos^2(2\alpha) + f \cos(\alpha) \sin(\alpha) \quad (4)$$

$$B(\alpha) = a_0 + b_0\theta^2 + a_1 \cos^2(\alpha) + \frac{a_2}{4} \cos^2(2\alpha) + f \cos(\alpha) \sin(\alpha) \quad (5)$$

$$C(\alpha) = a_1 \sin^2(\alpha) + \frac{a_2}{4} \sin^2(2\alpha) - f \cos(\alpha) \sin(\alpha) \quad (6)$$

Where $\Delta\varepsilon_P$ and $\Delta\varepsilon_A$ are the dielectric strength of phase and amplitude fluctuation modes respectively and corresponding frequencies are denoted by f_P and f_A . $A(\alpha)$, $B(\alpha)$, and $C(\alpha)$ are the elements of 2×2 matrix of change in free energy of the system due to fluctuation under harmonic external field. In Eq. (1) to (6), θ and α are the tilt angle magnitude and difference of the azimuthal angle between two smectic layers respectively, K' is a constant and γ is rotational viscosity. The parameters a_0 , b_0 , a_1 , a_2 are constant; however parameter f describe chirality of the systems.

3. EXPERIMENTAL

Different mesophase transition temperatures have been determined by using Differential Scanning Calorimeter (DSC) of Perkin-Elmer and a transmitted light polarizing microscope. The dielectric measurements have been carried out in the cell made from indium tin oxide (ITO) coated glass electrodes whose surfaces are chemically treated for planar and homeotropic orientation. Two plates of the cell have been separated by mylar spacers of thickness 5 and 10 μm . The dielectric data have been acquired with the help of impedance/gain-phase

analyser of Solartron (model SI-1260) coupled with Solartron dielectric interface (model-1296). A measuring ac voltage of $0.1 V_{\text{rms}}$ has been applied across the sample. In order to study the bias electric field dependence of dielectric parameters, a bias voltage of (0 to 40 V) has been superimposed on measuring ac electric field from SI-1260 bridge. Temperature of the sample has been controlled with the help of a hot stage of Instec (model HS-1) having accuracy of $\pm 0.1^\circ\text{C}$. Temperature near the sample has been determined by measuring thermo emf of a copper-constantan thermocouple with the help of a six and half digit multimeter with the accuracy of $\pm 0.1^\circ\text{C}$. Other details of experimental techniques have already been discussed elsewhere [15–17].

4. RESULTS AND DISCUSSION

4.1. Phase Transition

The investigated compound has following phase sequences in the heating and cooling cycles as obtained by DSC measurements at the scanning rate of $2.5^\circ\text{C}/\text{min}$.

Heating: Cr1 (63.8°C) Cr2 (70.5°C) SmC_α^* (74.0°C) SmA^* (100.0°C) Iso
Cooling: Iso (98.8°C) SmA^* (75.4°C) SmC_α^* (53.2°C) Cr2 (50.1°C) Cr1

In the cooling cycle material shows super cooling effect and crystallized below 53.2°C . Before acquiring the dielectric data, a good quality of molecular alignment has been ensured by cooling material very slowly ($0.05^\circ\text{C}/\text{min}$) from the isotropic liquid phase after filling it in the dielectric cells. Quality of the alignment has been confirmed under the polarizing microscope. In the present study, complete homogeneous alignment could not be possible for this material. $\text{SmA}^* - \text{SmC}_\alpha^*$ transition did not produce any drastic change in the texture and only a slight change in the colour of the texture has been observed. In principle, unwinding of helix lines should be observed in planar aligned sample of chiral tilted smectic phases. However the small pitch ($< 100 \text{ nm}$) of SmC_α^* phase make it very difficult to identify these lines [18]. It should be noted that in spite of tilt, the SmC_α^* phase is uniaxial and it is not easy to distinguish this phase from SmA^* phase on the basis of optical texture studies.

4.2. Dielectric Permittivity

The temperature dependence of dielectric permittivity (ϵ'_\perp) at various frequencies in the SmA^* and SmC_α^* phases are shown in Figure 2.

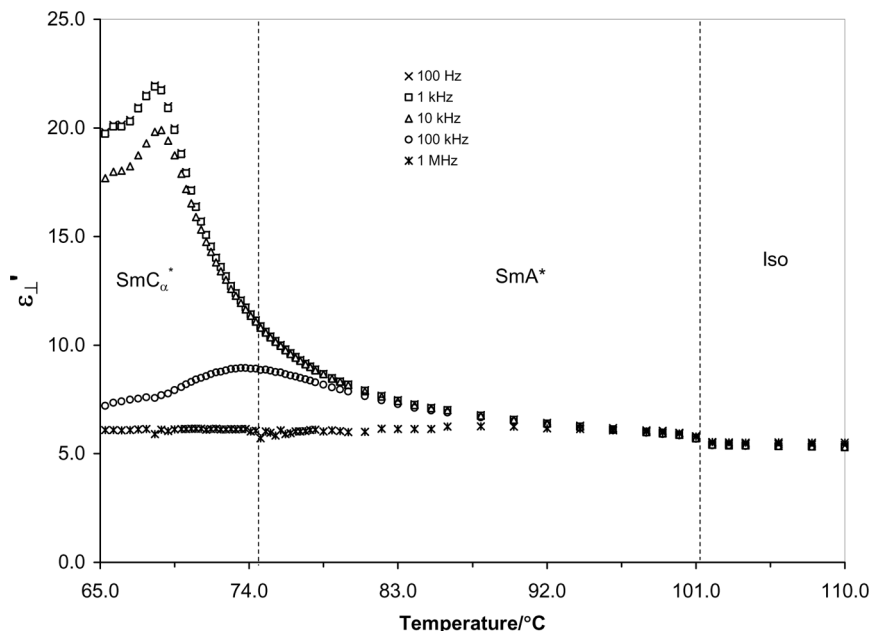


FIGURE 2 Temperature dependence of real part of dielectric permittivity (ϵ'_{\perp}) at different frequencies viz. 100 Hz (cross), 1 kHz (square), 10 kHz (triangle), 100 kHz (circle) and 1 MHz (asterisk) in the cooling cycle. Vertical broken line shows the separation of different phases on the basis of dielectric parameters.

In the isotropic phase the value ϵ'_{\perp} is found to be small (~ 5.2). At Iso--SmA* transition ϵ'_{\perp} increases slightly. Below Iso-SmA* transition the value of ϵ'_{\perp} is found to be (~ 6). It remains constant with temperature and frequency indicating no relaxation phenomenon in SmA* phase above $\sim 90^{\circ}\text{C}$. On lowering the temperature below 90°C , ϵ'_{\perp} is no more constant with frequency. This indicates the evolution of a relaxation process below 1 MHz. In the vicinity of SmA* – SmC $_{\alpha}^*$ transition, the value of ϵ'_{\perp} increases sharply at frequencies lower than 20 kHz and it saturates in SmC $_{\alpha}^*$ phase at $\sim 68.5^{\circ}\text{C}$. The maximum value of ϵ'_{\perp} is found to be ~ 22 at 100 Hz in the SmC $_{\alpha}^*$ phase. Below 100 Hz, value of ϵ'_{\perp} is affected due to low frequency artifacts as discussed in forthcoming section and increases sharply. It is important to mention here that the value of ϵ'_{\perp} is found to be of same order for other materials also [7,8]. Hoffmann *et al.* [7] have reported the maximum value of ϵ'_{\perp} about ~ 25 at 110 Hz in SmC $_{\alpha}^*$ phase for

MHPOPb. In the Cl-MHPOBC, the maximum value of ε'_{\perp} is found to vary between 20 and 40 at 100 Hz [8].

4.3 Dielectric Relaxation Modes

The measured dielectric absorption spectra at various temperatures of SmA^* and SmC_{α}^* phases are shown in Figure 3. To analyse the measured data, the dielectric spectra has been fitted with the help of generalised Cole-Cole equation [19,20]

$$\varepsilon^* = \varepsilon' - j\varepsilon'' = \varepsilon'(\infty) + \frac{\Delta\varepsilon}{1 + (j\omega\tau)^{(1-h)}} + \frac{A}{\omega^n} + \frac{\sigma_{\text{ion}}}{j\varepsilon_0\omega} - jB\omega^m \quad (7)$$

where $\varepsilon'(\infty)$ is high frequency limiting value of relative permittivity, $\Delta\varepsilon$, τ , and h are dielectric strength, the relaxation time (inverse of

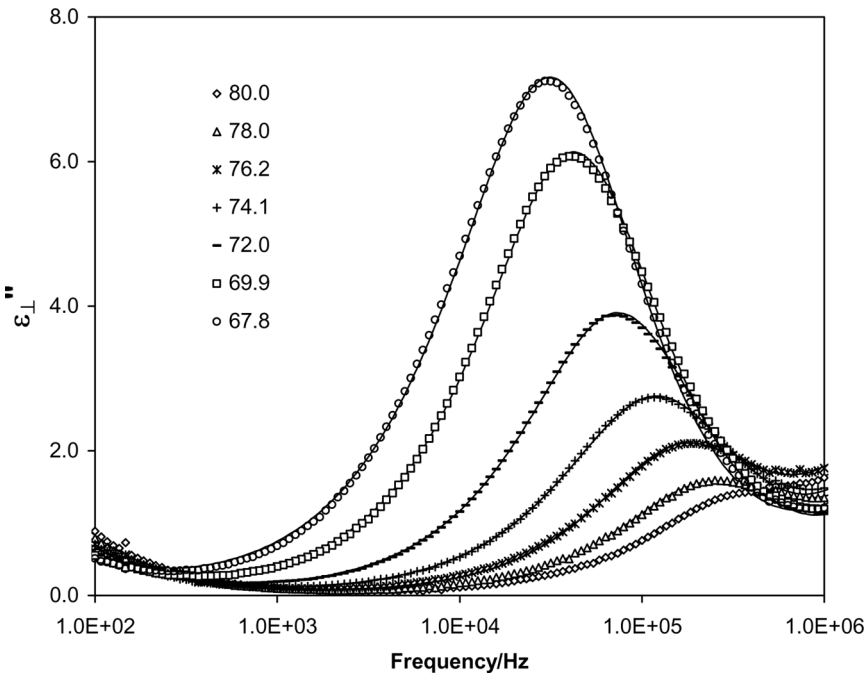


FIGURE 3 Dielectric absorption spectra at different temperatures in the SmA^* and SmC_{α}^* phases. The solid lines with experimental data represent the fitting of Eq. (7). Data below 100 Hz and above 1 MHz are highly affected due to low and high frequency effect hence not shown here in order to enhance the visualization of relaxation mode present in the material.

angular relaxation frequency) and symmetric distribution parameter ($0 \leq h \leq 1$) of relaxation mode respectively. The third and fourth terms in Eq. (7) are added due to the presence of electrode polarization capacitance and ionic conductance at low frequencies, where A and n are fitting constants [21,22]. σ_{ion} is the ionic conductance and ϵ_0 ($= 8.85 \text{ pF/m}$) is the free space permittivity. The fifth term is added in Eq. (7) to partially account for ITO resistance and lead inductances [22,23], where B and m are constants as for as correction terms are small.

The measured dielectric spectra are well described by single Cole-Cole type behaviour. The Cole-Cole plots of observed relaxation modes in SmA^* and SmC_α^* phases have been depicted in Figure 4. The data points lie on a semicircle except for those at low and high frequency sides. Low frequency effects due to ionic conductance are present up to $\sim 1 \text{ kHz}$ [21,22]. Data above 100 kHz are affected due to finite resistance of ITO sheet and lead inductances [22,23]. From Figure 4 it is evident that dielectric strength of the relaxation mode observed in SmA^* phase, increases significantly in SmC_α^* phase. Distribution parameter (h) calculated with the help of Cole-Cole plot in SmA^* phase has been found to be approximately zero, which indicates that this relaxation mode arises due to single molecular phenomena while in the case of SmC_α^* phase, the value of h lies between 0.05 and 0.2 which shows quasi-dispersive nature of relaxation process [8].

The dielectric strength ($\Delta\epsilon$), and relaxation frequency (f_R) of the observed mode for SmA^* and SmC_α^* phases are shown in Figures 5 and 6 respectively for sample thickness 5 and $10 \mu\text{m}$. The value of $\Delta\epsilon$ and f_R are found to be approximately same for two cell thicknesses. The relaxation frequency of the observed mode for SmA^* phase decreases continuously with decrease in temperature whereas the dielectric strength shows opposite trend. Taking into account of the molecular structure of SmA^* phase and its temperature dependence, this mode must correspond to amplitude mode (so-called soft mode) which is associated with director tilt fluctuation of molecules in the smectic layers [8,11,24].

At $\text{SmA}^* - \text{SmC}_\alpha^*$ transitions, a clear change in the slope of relaxation frequency and inverse dielectric strength have been observed for sample thickness $10 \mu\text{m}$ (see Figs. 5 and 6). However, this change is less pronounced for the cell thickness $5 \mu\text{m}$. A sharp increase in the value of distribution parameters has also been found at $\text{SmA}^* - \text{SmC}_\alpha^*$ transition as evidenced from Figure 4(b). High value of h in SmC_α^* phase i.e., broadening of the relaxation peak as compared to orthogonal SmA^* phase may be assigned to the tilting of molecules in SmC_α^* phase. On lowering temperature of the sample in the SmC_α^*

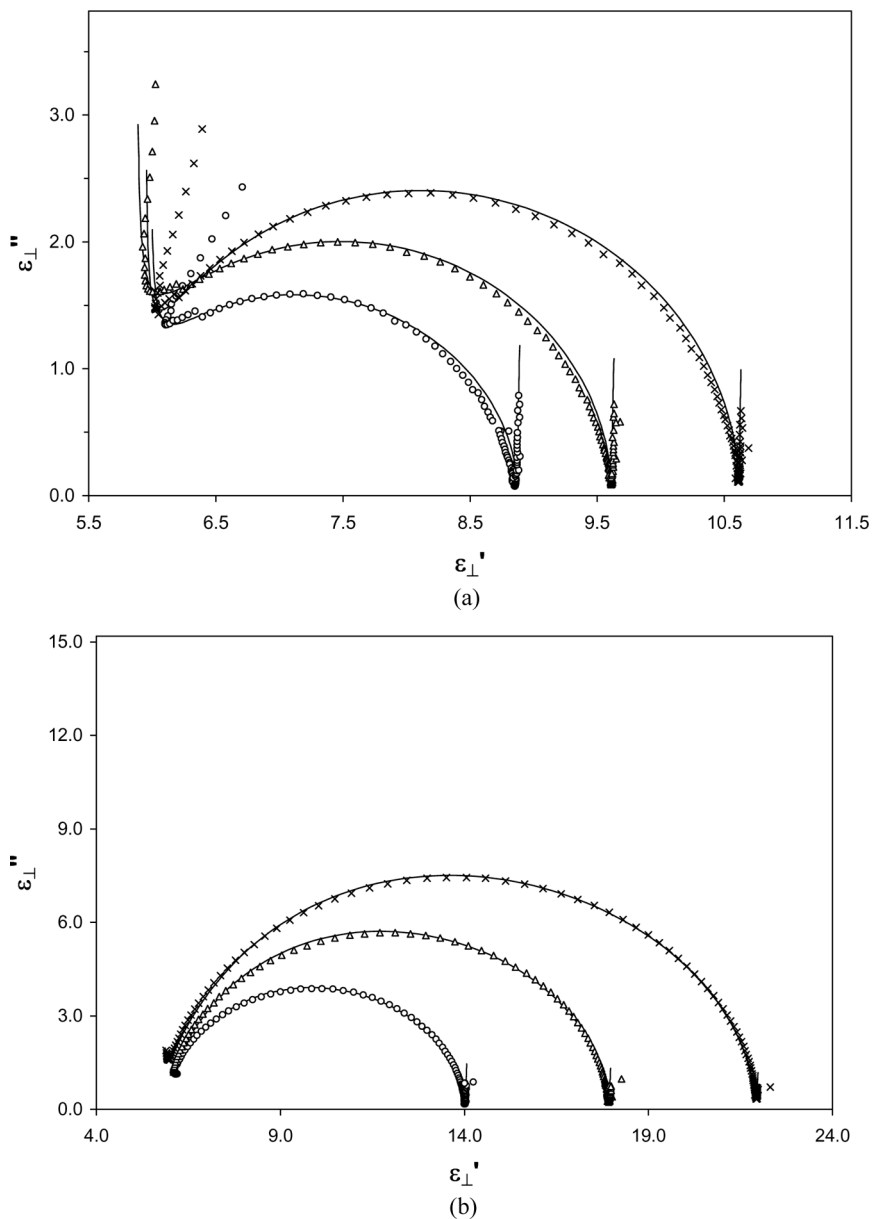


FIGURE 4 Cole-Cole arcs in (a) SmA* phase at 78°C (circle), 76.5°C (triangle) and 75°C (cross) and (b) SmC*_α phase at 74.1 (circle), 72.0 (triangle), 70.2 (cross) and 68.3°C (doubles). Solid line with the experimental data shows best fitting of Eq. (7).

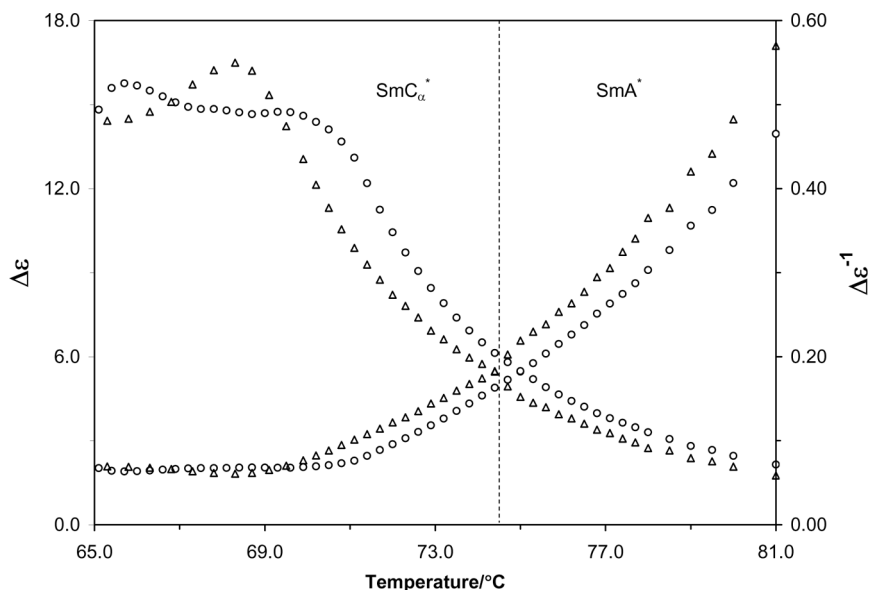


FIGURE 5 Temperature dependence of dielectric strength ($\Delta\epsilon$) and inverse of dielectric strength ($\Delta\epsilon^{-1}$) of SmA^* and SmC_α^* phases in cooling cycle for sample thickness $5\mu\text{m}$ (open circle) and $10\mu\text{m}$ (open triangle). Vertical broken line shows the separation of two phases on the basis of dielectric parameters.

phase, f_R decreases moderately and $\Delta\epsilon$ increases sharply (see Figs. 5 and 6). Below 69.0°C in the SmC_α^* phase, f_R becomes invariant with temperature and $\Delta\epsilon$ decreases slowly with decrease in temperature. In the case of cell thickness $5\mu\text{m}$ the behaviour of f_R changes at $\sim 71.0^\circ\text{C}$. It is worthwhile to mention here that below 70°C , SmC_α^* phase exists due to super cooling. Hence two different behaviour of dielectric parameters in the SmC_α^* phase are not surprising.

Figure 7 shows dielectric absorption spectra at 72.0 and 70.0°C with bias electric field varying from 0 to 36.0 kV/cm . It has been found that relaxation frequency and dielectric strength of the observed mode are not affected up to 6 kV/cm . On increasing the field above 6 kV/cm , dielectric strength decreases slowly. Shift in the relaxation frequencies has also been observed above 12 kV/cm (see Fig. 7). This behaviour is clearly seen from Figure 8 which shows variation of f_R and $\Delta\epsilon$ with bias electric field at three temperatures 74.0 , 72.0 , and 70.0°C respectively. From Figure 8, one can see that f_R and $\Delta\epsilon$ of the observed mode of SmC_α^* phase is less affected near $\text{SmA}^* - \text{SmC}_\alpha^*$ transition. However appreciable change in the magnitude of f_R and $\Delta\epsilon$ have been found far from transition.

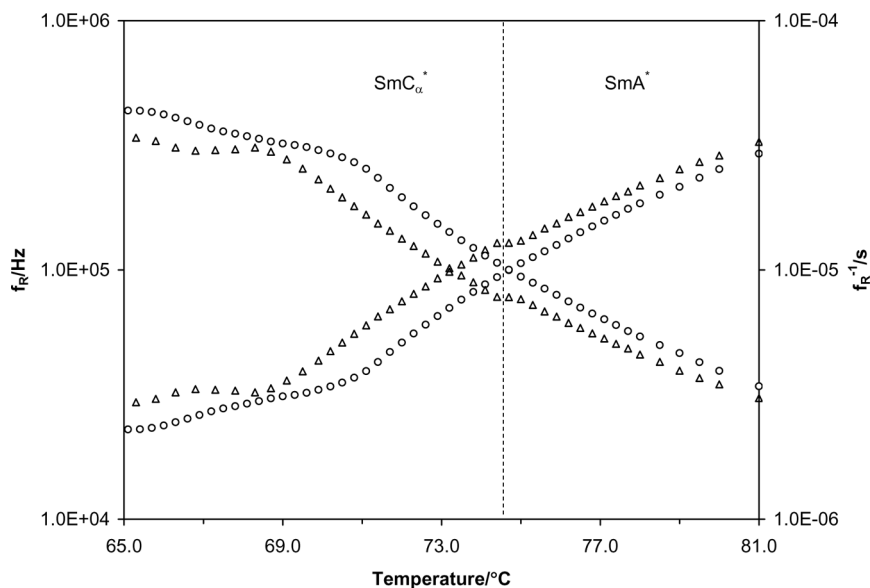


FIGURE 6 Temperature dependence of relaxation frequencies (f_R) and inverse relaxation frequencies (f_R^{-1}) in SmA^* and SmC_α^* phases in the cooling cycle for sample thickness $5\ \mu\text{m}$ (open circle) and $10\ \mu\text{m}$ (open triangle). Vertical broken line shows the separation of two phases on the basis of dielectric parameters.

Investigation of molecular relaxation process has been carried out for homeotropic orientation of molecules (thickness $10\ \mu\text{m}$). Completely dark field of view has been observed in smectic phases only after shearing two glass plates below the isotropic to SmA^* transition [25,26]. Only one relaxation mode has been observed in the dielectric spectrum of SmA^* and SmC_α^* phases. The relaxation frequency of observed mode shows strong temperature dependence and its dielectric strength remains invariant with temperature. The relaxation frequencies follow Arrhenius behaviour in SmA^* and SmC_α^* phases as shown in Figure 9. On the basis of temperature dependence, its origin has been stipulated due to reorientation of molecules about their short axes. Least square fit of $\ln(f_{R\parallel})$ with $1000/T$ gives straight line and hence, activation energies (W_a) corresponding to SmA^* and SmC_α^* phases have been calculated. Activation energies are found to be $79.5\ \text{kJ/mol}$ and $76.4\ \text{kJ/mol}$ in SmA^* and SmC_α^* phases respectively.

Now we come to expected origin of collective relaxation mode in SmC_α^* phase. In general single relaxation mode is reported for SmC_α^* phase in the literature [4–9]. Its relaxation frequency varies

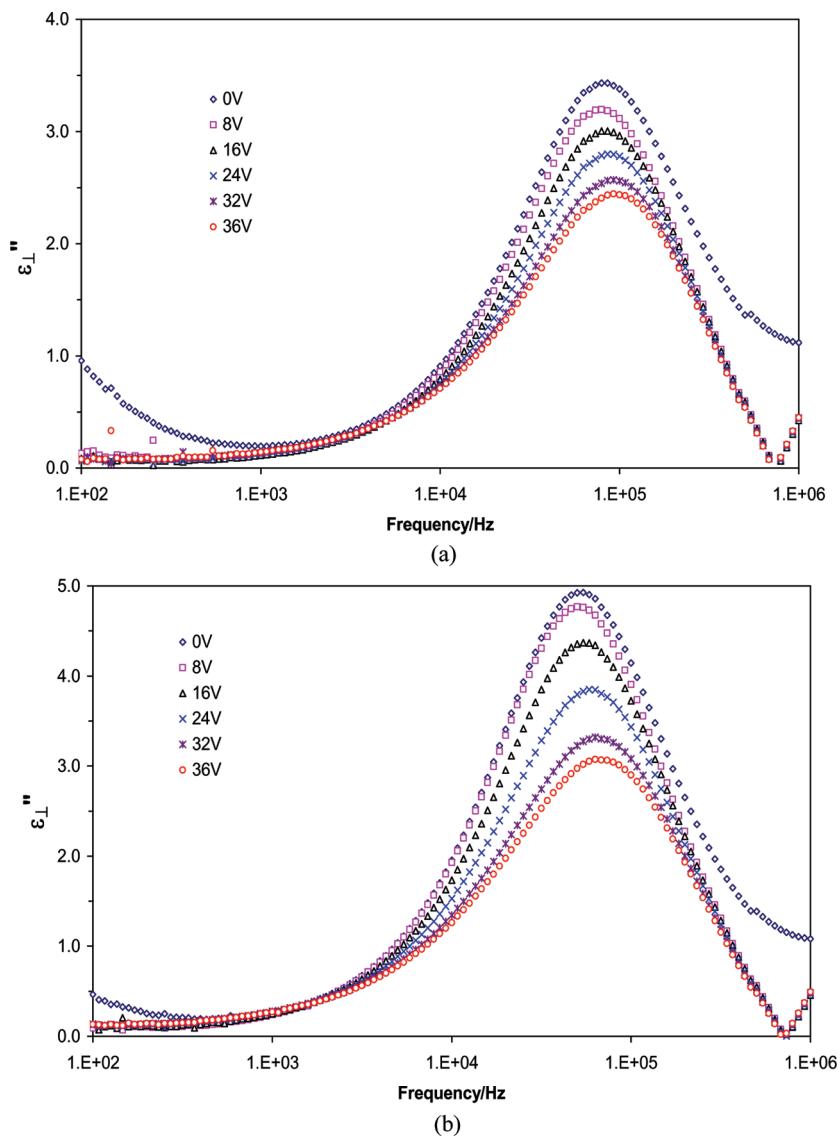


FIGURE 7 Effect of bias electric field on dielectric absorption spectra in SmC_α^* phase at 72.0 and 70.0°C for the sample thickness of $10\mu\text{m}$.

in a fashion similar to that of the soft mode of SmA^* phase but slope for the variation has been found to be different in two cases [4,8]. Hence the relaxation mode observed for SmC_α^* phase is assigned to

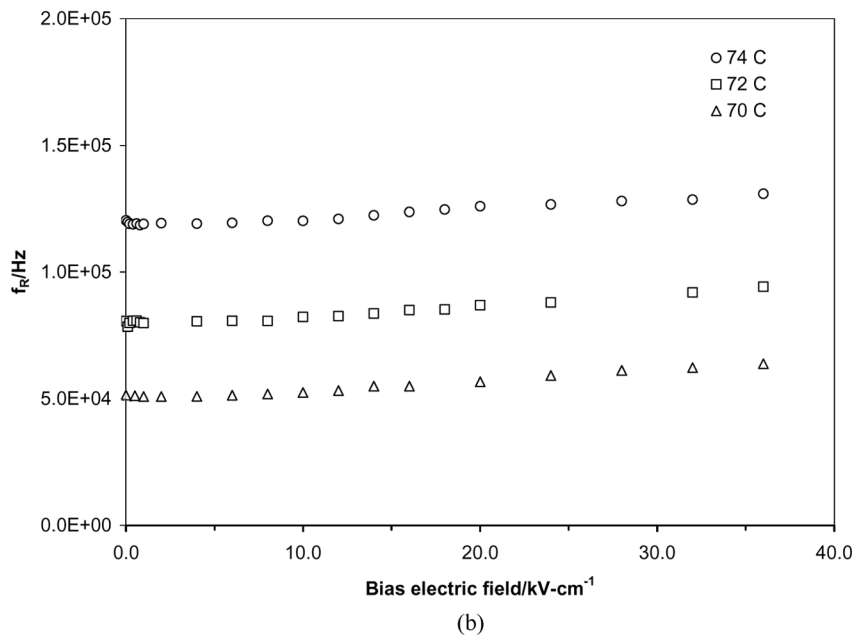
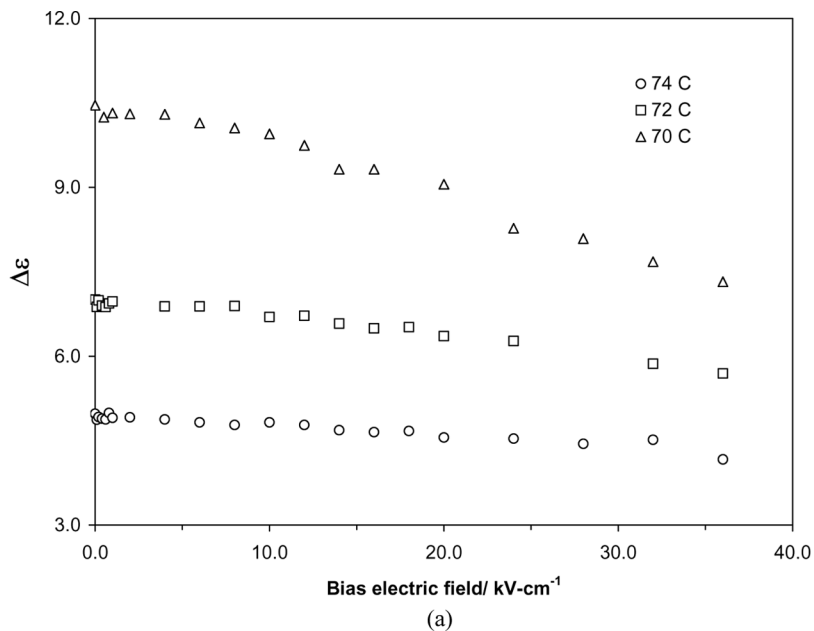


FIGURE 8 Variation of (a) dielectric strength ($\Delta\epsilon$) and (b) relaxation frequency (f_R) with bias electric field at 74.0, 72.0, and 70.0°C.

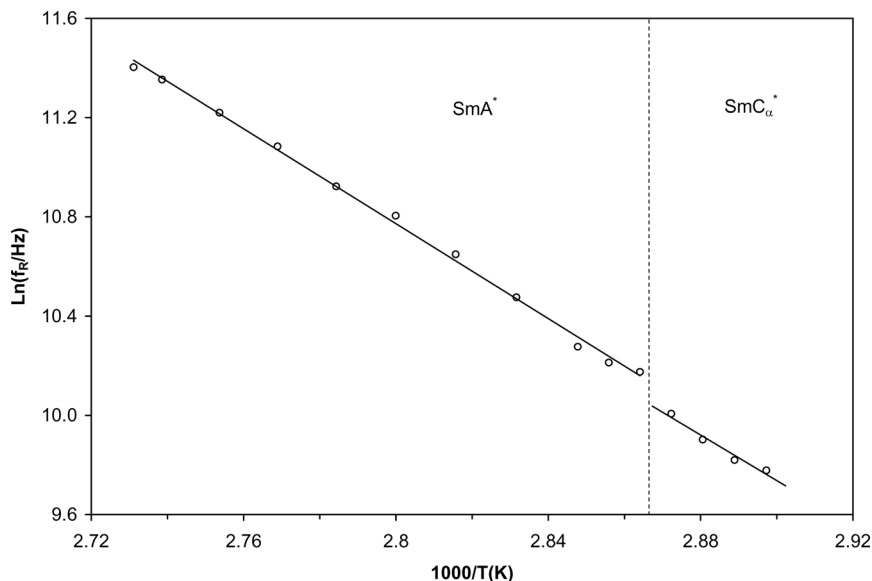


FIGURE 9 Arrhenius plot of relaxation mode observed under homeotropic anchoring of molecules for thickness $10\ \mu\text{m}$. Vertical broken line shows the separation of two phases on the basis of dielectric parameters.

ferroelectric soft mode. According to theory of Vaupotic *et al.* two dielectric relaxation processes namely amplitude and phase fluctuation modes should be observed in dielectric spectrum of SmC_α^* phase. This work has been further extended by Douali *et al.* by numerical simulations to describe the behaviour of experimentally observed relaxation mode in SmC_α^* phase for different values of azimuthal angle difference (α) between two successive smectic layers [12]. They have found that the only possibility to explain the observed temperature and frequency dependence of dielectric modes in SmC_α^* phase is the existence of two modes as predicted by theory. On the basis of their simulation results and experimental observation, they have shown that Goldstone mode will be dominant for low value of α ($<25^\circ$). In this case soft mode can not be observed without application of bias electric field. When the value of α increases, the dielectric strength of the Goldstone mode decreases and the soft mode contribution is predominant in the vicinity of $\text{SmA}^* - \text{SmC}_\alpha^*$ transition. From temperature dependence study, we have observed that f_R decreases with decrease in temperature below $\text{SmA}^* - \text{SmC}_\alpha^*$ transition. However f_R remains unaffected at low electric field and increases slowly above $12\ \text{kV/cm}$.

This suggests soft mode behaviour of observed relaxation mechanism near to $\text{SmA}^* - \text{SmC}_\alpha^*$ transition. On lowering the temperature below 71°C (in case of cell thickness $5\ \mu\text{m}$), f_R becomes constant and $\Delta\varepsilon$ indicates saturation behaviour with temperature. This indicates different nature of relaxation mechanism to that observed near $\text{SmA}^* - \text{SmC}_\alpha^*$ transition. This is the signature of Goldstone like mode of SmC_α^* . One may argue that Goldstone mode frequency should not be so high. It should be noted that relaxation frequency of Goldstone mode is inversely proportional to square of helical pitch and rotational viscosity [8,13]. As the pitch in the SmC_α^* phase is found to be very small ($\sim 30\text{--}80\ \text{nm}$) [18], it is expected that frequency of Goldstone mode in SmC_α^* phase may be high in comparison to usual SmC^* phase. Hence in the present case, two different behaviour of relaxation process of SmC_α^* phase are stipulated due to amplitude and phase fluctuations (soft and Goldstone like mode) respectively.

CONCLUSIONS

The investigated compound (S)-(+)-4-(1-methylheptyl) 4-[4-(3-hexanoyloxyprop-1-oxy)benzoyloxy]biphenylate shows exceptionally wide temperature range SmC_α^* phase of $\sim 9^\circ\text{C}$. A soft mode relaxation has been observed for SmA^* phase for planar oriented samples. This relaxation mode has also been observed in the SmC_α^* phase, but behaviour is found to be different to those of SmA^* phase. The observed behaviour of this mode has been compared with theoretical models. It has been found that this mode shows different characteristic in two temperature ranges. Near $\text{SmA}^* - \text{SmC}_\alpha^*$ transition, it behaves like soft mode. However far from transition, it behaves as Goldstone like mode. A mode of relaxation has also been observed for SmA^* and SmC_α^* phases under homeotropic anchoring of samples due to reorientation of molecules around short axis.

REFERENCES

- [1] Musevic, I., Blinc, R., & Zeks, B. (2000). *The Physics of Ferroelectric and Antiferroelectric Liquid Crystals*, World Scientific: Singapore.
- [2] Mach, P., Pindak, R., Levelut, A. M., Barois, P., Nguyen, H. T., Huang, C. C., & Furenlid, L. (1998). *Phys. Rev. Lett.*, *81*, 1015.
- [3] Liu, Z. Q., McCoy, B. K., Wang, S. T., Pindak, R., Caliebe, W., Barois, P., Fernandes, P., Nguyen, H. T., Hsu, C. S., Wang, S., & Huang, C. C. (2007). *Phys. Rev. Lett.*, *99*, 077802.
- [4] Cepic, M., Heppke, G., Hollidt, J. M., Lotzsch, D., Moro, D., & Zeks, B. (1995). *Mol. Cryst. Liq. Cryst.*, *263*, 207.

- [5] Merino, S., de la Fuente, M. R., Gonzalez, Y., Perez Jubindo, M. A., Ros, B., & Puertolas, J. A. (1996). *Phys. Rev. E*, 54, 5169.
- [6] Fafara, A., Wrobel, S., Haase, W., Marzec, M., & Dabrowski, R. (2002). *SPIE*, 4759, 151.
- [7] Hoffmann, J., Giesselmann, F., & Kuczynski, W. (2007). *Phase Transitions*, 80, 841.
- [8] Pandey, M. B., Dhar, R., Agrawal, V. K., Dabrowski, R., & Tykarska, M. (2004). *Liq. Cryst.*, 31, 973.
- [9] Hou, J., Schacht, J., Giesselmann, F., & Zugenmaier, P. (1997). *Liq. Cryst.*, 22, 409.
- [10] Vaupotic, N., Cepic, M., & Zeks, B. (2000). *Ferroelectrics*, 245, 175.
- [11] Pandey, M. B., Dhar, R., & Dabrowski, R. (2008). *Liq. Cryst.*, 35, 777.
- [12] Douali, R., Legrand, C., Laux, V., Isaert, N., Joly, G., & Nguyen, H. T. (2004). *Phys. Rev. E*, 69, 031709.
- [13] Pandey, M. B., Dhar, R., & Dabrowski, R. (2008). *J. Physics Condens. Matter*, 20, 115207.
- [14] Gasowska, J. (2004). Chiral and achiral high tilted synclinic and antclinic smectics, PhD dissertation, Military University of Technology, Warsaw Poland.
- [15] Pandey, M. B., Dhar, R., Agrawal, V. K., Khare, R. P., & Dabrowski, R. (2003). *Phase Transitions*, 76, 945.
- [16] Pandey, M. B., Dhar, R., Agrawal, V. K., & Dabrowski, R. (2004). *Mol. Cryst. Liq. Cryst.*, 414, 63.
- [17] Pandey, M. B., Dabrowski, R., & Dhar, R. (2007). *Physica B*, 387, 25.
- [18] Ortega, J., Folcia, C. L., Etxebarria, J., & Ros, M. B. (2003). *Liq. Cryst.*, 30, 109.
- [19] Cole, K. S. & Cole, R. H. (1941). *J. Chem. Phys.*, 9, 341.
- [20] Pandey, M. B., Dhar, R., & Dabrowski, R. (2006). *Ferroelectrics*, 343, 83.
- [21] Srivastava, S. L. & Dhar, R. (1991). *Ind. J. Pure Appl. Phys.*, 29, 745.
- [22] Gouda, F. M., Skarp, K., & Lagerwall, S. T. (1991). *Ferroelectrics*, 113, 165.
- [23] (a) Srivastava, S. L. (1993). *Proc. Nat. Acad. Sci. India*, 63, 311; (b) Dhar, R. (2004). *Ind. J. Pure Appl. Phys.*, 42, 56.
- [24] Pandey, M. B., Dhar, R., & Dabrowski, R. (2008). *Phil. Magazine*, 88, 101.
- [25] Pandey, M. B., Dhar, R., Agrawal, V. K., & Dabrowski, R. (2005). *Phase Transitions*, 78, 457.
- [26] Pandey, M. B., Dhar, R., & Dabrowski, R. (2006). *mySCIENCE. A Journal of the University of Mysore, India*, 1(2), 135.